JOURNAL OF CATALYSIS **159,** 50–57 (1996)
ARTICLE NO. 0063

Interaction of CO with Rh Supported on Stoichiometric and Reduced $CeO_2(111)$ and $CeO_2(100)$ Surfaces

J. Stubenrauch and J. M. Vohs

Department of Chemical Engineering and Laboratory for Research on the Structure of Matter, University of Pennsylvania, Philadelphia, Pennsylvania 19104

Received March 10, 1995; revised October 16, 1995; accepted October 20, 1995

The structure and reactivity of Rh films supported on the surface of a CeO_2 single crystal were studied using Auger electron spectroscopy (AES) and temperature-programmed desorption (TPD). Rhodium films deposited from the vapor phase were found to grow via the nucleation of three-dimensional particles at a sample temperature of 300 K. Annealing of the Rh films resulted in further agglomeration of the metal layer. Carbon monoxide TPD spectra obtained from Rh supported on oxygen-annealed $CeO_2(111)$ and $CeO_2(100)$ substrates were similar to those obtained from the low-index planes of Rh single crystals, with the exception that a small fraction of the CO (ca. 2%) was oxidized to CO_2. In contrast, a new high-temperature CO desorption state was observed in the TPD spectra obtained from Rh supported on partially reduced CeO_2 surfaces.

INTRODUCTION

It is well known that the addition of CeO_2 improves the performance of Group VIII metal-based three-way catalysts for automobile exhaust emissions control. Although the role of ceria in these catalysts is still a subject of intense investigation, it appears that ceria may improve catalytic performance via several mechanisms. These include, enhancement of the activity for the water–gas shift reaction (1), stabilization of the γ-Al_2O_3 support and the noble metal dispersion, and the ability to store and release oxygen (2–6). It has also been proposed that interactions between ceria and noble metals may result in an enhancement of the CO oxidation activity of the metal (7–9).

Recently, in an effort to elucidate how interactions between CeO_2 and Rh affect catalytic performance, several research groups have used surface science techniques to study the reactivity of well-defined model catalysts (8–12). The most extensive of these investigations are those of Zafiris and Gorte (8, 9). These researchers studied the reactivity of model catalysts composed of Rh films vapor deposited on planar, low surface area films of polycrystalline CeO_2. They found that for CO-dosed Rh/CeO_2, a significant fraction of the adsorbed CO was oxidized to CO_2 during temperature-programmed desorption (TPD) experiments. Based on this result, it was concluded that oxygen from the surface region of the CeO_2 support was able to migrate onto the Rh particles at temperatures greater than 400 K and react with adsorbed CO. Studies of the reaction of NO on Rh/CeO_2 provided additional evidence for this conclusion. Zafiris and Gorte proposed that the ability of oxygen to migrate from CeO_2 to Rh explains the high activity of Rh/CeO_2 catalysts for the water–gas shift reaction (8, 9).

Several studies of model catalysts composed of films or particles of CeO_2 supported on Rh foils or single crystals can also be found in the literature (13–19). For example, Belton and Schmieg used XPS to study the oxidation and reduction of CeO_2 particles supported on Rh(111) (14). They concluded that intimate contact between Rh and CeO_2 enhances the reduction of CeO_2 during reaction with CO. Similar studies have been performed by Marbrow and Lambert for microcrystallites of CeO_2 supported on a Rh foil (18). They also found that CO was oxidized to CO_2 during TPD experiments with the oxygen being supplied via reduction of the CeO_2.

In the work described here, we have expanded on the previous studies employing model Rh/CeO_2 catalysts to investigate the structure and reactivity of Rh films supported on $CeO_2(111)$ and $CeO_2(100)$ surfaces. As will be shown below, the results of this study indicate that the structure of the CeO_2 surface, specifically its degree of reduction, can influence the interaction of CO with supported Rh particles.

EXPERIMENTAL

Experiments were conducted in three separate ultra-high-vacuum surface analysis systems. Each system was equipped with a quadrupole mass spectrometer (UTI) and an ion sputter gun. One of the systems contained a retarding field electron energy analyzer (Omicron) for LEED studies, while another contained a cylindrical mirror analyzer (Omicron) for AES experiments. The XPS spectra were obtained in a chamber equipped with a hemispherical

0021-9512/96 $18.00

electron energy analyzer and an Al $K\alpha$ X-ray source (VG Scientific).

The CeO_2 single-crystal substrate used in this study was approximately $7 \times 4 \times 1$ mm in size and was cut from a large macroscopic CeO_2 single crystal obtained from Commercial Crystal Laboratories. Prior to being cut, the crystal was oriented to expose the (111) surface using Laue X-ray diffraction. The surface of the sample was polished until optically smooth by the manufacturer using a proprietary method. The CeO_2(100) substrate was obtained from Los Alamos National Laboratory and consisted of an epitaxial film of CeO_2 deposited on *r*-plane sapphire. The film was grown using 90° off-axis RF magnetron sputtering with a gas phase consisting of 60% Ar and 40% O_2 at a total pressure of 4×10^{-2} Torr. The average thickness of the film was 100 Å and the orientation was verified using X-ray diffraction. AFM analysis of the surface of the film indicated that it was composed of crystalline domains with lateral dimensions of approximately 1000×1000 Å.

The CeO_2(111) and CeO_2(100) samples were mounted in tantalum holders which in turn were attached to an electrical feedthrough on a UHV sample manipulator. The samples could be heated in excess of 950 K and cooled to 180 K via conduction from the sample holder. The temperature was monitored using a chromel-alumel thermocouple which was attached to the back face of the samples using a ceramic adhesive (Aremco No. 516).

Once in vacuum, the surface of the CeO_2(111) sample was cleaned by sputtering with 500 eV Ar^+ ions for 30 min followed by annealing at 800 K in 1×10^{-7} Torr of O_2 for 1 h. This sputter/anneal cycle was repeated until a clean, well-ordered CeO_2(111) surface was obtained as determined by LEED and AES. A portion of the experiments were performed with CeO_2(111) surfaces which had been lightly sputtered. These surfaces were prepared as described above and then sputtered for an additional 15 min with 500 eV Ar^+ ions followed by momentarily heating to 800 K. The CeO_2(100) epitaxial film was cleaned by annealing in 1×10^{-7} Torr of O_2 for 1 h. The cleanliness of this surface was also monitored using AES. The insulating nature of the sapphire substrate precluded LEED analysis of the CeO_2(100) surface.

Rhodium was deposited on the CeO_2(111) and CeO_2(100) surfaces using an evaporative metal source. The source consisted of a 0.25 mm-diameter tungsten wire wrapped with a small piece of 0.127 mm-diameter Rh wire (Johnson Matthey, 99.8% purity). The tungsten wire was attached to an electrical feedthrough on the UHV system allowing it to be heated resistively. The source was operated with a steady-state flux of Rh atoms of 3.5×10^{12} atoms/cm · s as determined by a quartz crystal film thickness monitor. The Rh coverage was measured in monolayers (ML) where one monolayer was defined to be 1.6×10^{15} atoms/cm^2, the density of atoms in a close-packed plane of Rh. All metal depositions were performed at a sample temperature of 300 K.

During TPD experiments the sample heating rate (4 K/s) was controlled using a microcomputer. The computer was also used to multiplex the mass spectrometer, allowing multiple *m*/*e* values to be monitored during each TPD experiment. Saturation exposures of CO (Matheson, 99.9% purity) were used in all TPD experiments.

RESULTS

Characterization of CeO_2(111) and CeO_2(100)

The sputtered and annealed CeO_2(111) surface exhibited a sharp hexagonal LEED pattern. This symmetry is consistent with that expected for the (111) plane of an ideally terminated fluorite crystal lattice. A model of the ideal surface is displayed in Fig. 1. This surface is terminated by O^{-2} anions and a subsurface layer of Ce^{+4} cations. Both the surface cations and anions are each deficient one nearest neighbor in their respective coordination spheres (note, other terminations parallel to the (111) plane are also possible, but result in surfaces composed of cations and anions which have multiple coordination vacancies and are presumably less stable than the surface depicted in Fig. 1). The CeO_2(100) surface also has both cations and anions exposed. The oxygen anions, however, are fully coordinated, while the cerium cations have four coordination vacancies. A model of this surface is also depicted in Fig. 1.

XPS was used to determine the oxidation state of the surface Ce cations. Figure 2 displays Ce(3*d*) spectra for both the freshly annealed (111) surface and the same surface after sputtering with 500 eV Ar^+ ions for 15 min and briefly flashing to 800 K. The spectrum of the annealed surface is quite complex and contains two broad regions of overlapping peaks, one located between 877 and 890 eV and a second between 895 and 910 eV. An additional peak is also observed at 916 eV. An identical spectrum was obtained from samples that were not exposed to O_2 during annealing (i.e., annealed in vacuum). The spectrum is similar to that which has been reported previously for completely oxidized polycrystalline CeO_2 (20, 21). The complexity of the spectrum is a result of final state effects. Based on the work of Creaser *et al.*, the spectrum can be assigned to four sets of doublets (21). The peaks labeled u result from $3d_{5/2}$ emissions, while the corresponding $3d_{3/2}$ emissions are labeled v. Peaks u‴ and v‴ have been assigned to primary photoemissions from Ce^{+4} cations, while the remaining three doublets correspond to different shakedown features (20, 21).

The Ce(3*d*) spectrum of the sputtered CeO_2(111) surface is shown in the lower portion of Fig. 2. Comparison of this spectrum to that of the annealed surface reveals several differences, the most important being a change in the relative intensities of the various peaks. The large decrease in the

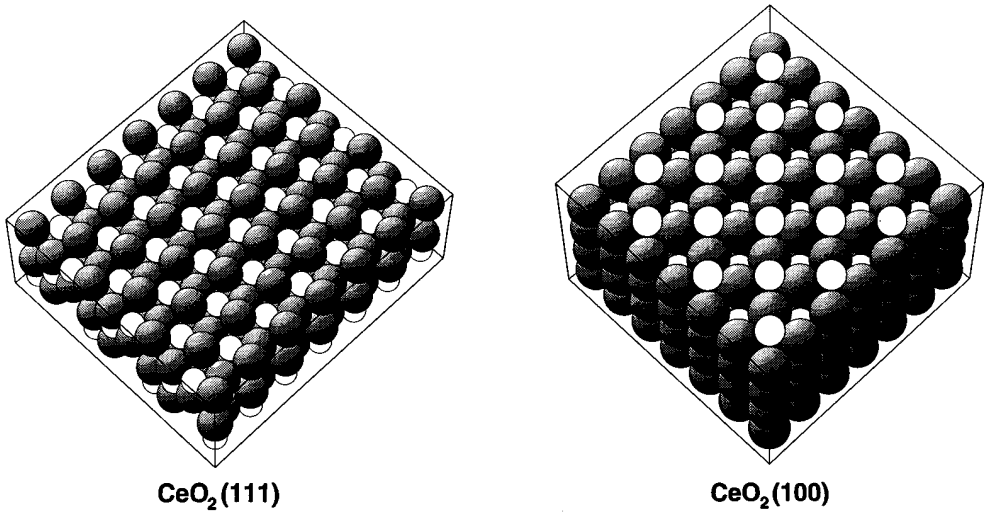

FIG. 1. Model of the CeO_2 lattice showing the (111) and (100) surfaces. The small white balls correspond to Ce^{+4} cations, while the large black balls correspond to O^{-2} anions.

intensity of the primary photoemission peaks from Ce^{+4} cations (i.e., peaks v‴ and u‴) indicates a partial reduction of the surface. Due to the complexity of the Ce(3*d*) spectrum and the fact that the XPS sampling depth is 30–40 Å, it is difficult to quantify the degree of surface reduction. Comparison to the detailed XPS study of polycrystalline ceria by Creaser *et al.* (21) suggests, however, that the stoichiometry of the near surface region of the sputtered sample is approximately $CeO_{1.75}$. This result is consistent with the preferential removal of oxygen while sputtering and indicates that the surface contains Ce cations in both $+3$ and $+4$ oxidation states. XPS spectra were also collected for the CeO_2(100) thin film following annealing in vacuum and in oxygen. In both cases, the Ce(3*d*) spectra were similar to that obtained from the sputtered CeO_2(111) surface.

Rh Films on CeO_2(111) and CeO_2(100)

The growth of Rh films on CeO_2(111) was initially studied using AES. Figure 3 displays the relative intensities of the Rh(MNN), Ce(MNN), and O(KLL) Auger peaks as a function of the amount of Rh deposited on the oxygen-annealed CeO_2(111) surface. The intensity of the Ce and O peaks decreased relatively slowly with increasing Rh coverage. For a Rh coverage of 3 ML, the Ce and O peak intensities were 0.58 and 0.40 of that obtained from the clean surface. Similar trends were observed for the CeO_2(100) substrate. Although it is difficult to discern film growth modes using AES data alone, the rather slow diminution of the substrate peaks suggests that the film does not grow in a layer-by-layer fashion. The results of HREELS experiments, which will be published separately (22), were consistent with this

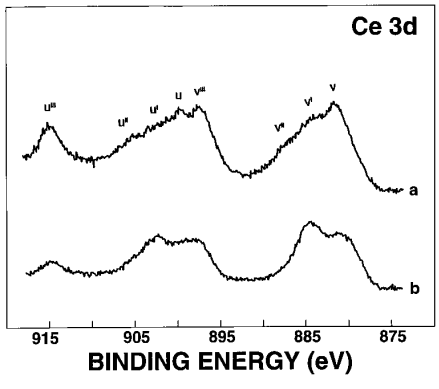

FIG. 2. Ce(3*d*) XPS spectrum of (a) CeO_2(111) prepared by sputtering and then annealing at 800 K in 1×10^{-7} Torr of O_2 for 1 h, and (b) the surface in (a) after sputtering with Ar^+ for 15 min.

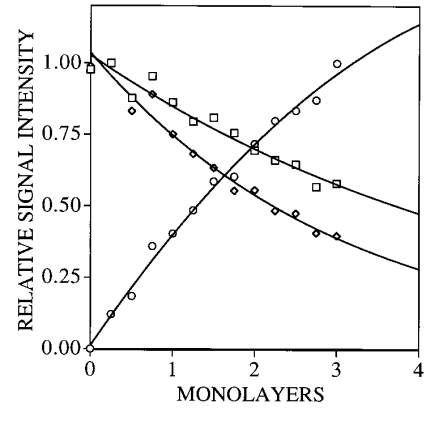

FIG. 3. Rh(MNN) (◯), O(KLL) (◇), and Ce(MNN) (□) AES peak intensities as a function of Rh coverage. The substrate signal intensities have been normalized to that obtained from the clean surface. The Rh signal intensity was normalized to that obtained for a Rh coverage of 3 ML.

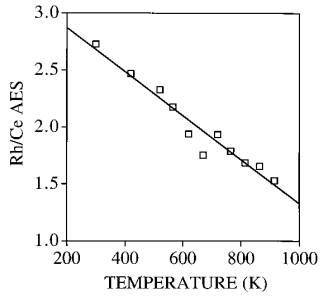

FIG. 4. Rh(MNN)/Ce(MNN) AES peak intensity ratio as a function of temperature for a 3 ML Rh film on CeO_2(111).

conclusion and indicated growth via nucleation of three-dimensional particles (i.e., a Volmer-Weber growth mode).

The thermal stability of a 3 ML Rh layer on the CeO_2(111) surface was also studied using AES. In this set of experiments the sample was heated to the temperature of interest and then rapidly quenched to 300 K at which point an AES spectrum was collected. In Fig. 4, the ratio of the intensity of the Rh AES signal to that of Ce is plotted as a function of the annealing temperature. The Rh/Ce ratio decreases in a nearly linear fashion for temperatures up to 920 K, indicating that sintering of the Rh layer into larger particles occurred as the temperature was increased. This result is consistent with that obtained by Zafiris and Gorte for Rh deposited on polycrystalline CeO_2 (23).

Interaction of CO with Rh/CeO_2(111) and Rh/CeO_2(100)

A series of TPD spectra obtained from CO-dosed Rh/CeO_2(111) are displayed in Fig. 5. The sample used in these experiments was prepared by depositing 3 ML of Rh on the oxygen-annealed CeO_2(111) surface at 300 K. The top spectra in the upper and lower portions of the figure correspond to the CO and CO_2 desorption curves, respectively, obtained from the freshly deposited Rh layer. The final temperature of this TPD run was 600 K. Successive TPD experiments were performed with increasing final temperatures. This was done in order to study the effect of annealing temperature on the TPD results. The temperature label for each spectrum in this figure corresponds to the highest temperature that the sample had been subjected to prior to that experiment. It should be noted that CO TPD experiments performed prior to metal deposition demonstrated that CO does not adsorb on the clean CeO_2(111) and CeO_2(100) surfaces under ultra-high vacuum conditions. Thus, the features in Fig. 5 can be attributed to CO adsorbed on the metal particles.

The data in the upper portion of Fig. 5 show that CO desorbed from the as-deposited 3 ML Rh film in an asymmetric peak centered at 500 K. The smaller peak at 330 K is due to desorption of CO from the crystal support hardware. The CO peak temperature and shape is the same as that reported for the desorption of CO from the low index

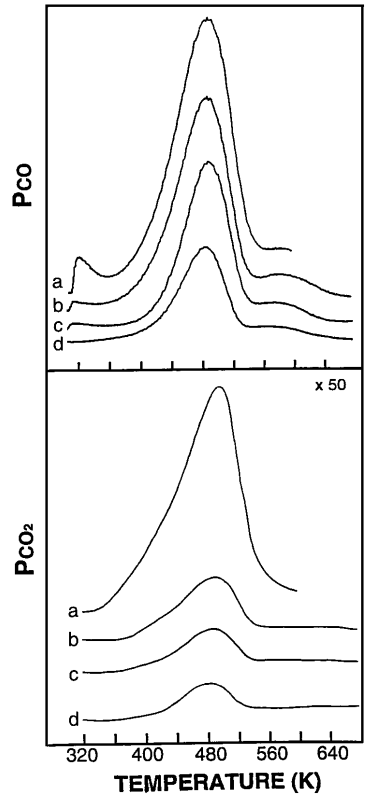

FIG. 5. TPD spectra following CO adsorption at 300 K on the 3 ML Rh film supported on the oxidized CeO_2(111) sample. The upper and lower panels correspond to CO and CO_2 desorption spectra, respectively, obtained after the sample had been heated to (a) 300, (b) 600, (c) 750, and (d) 950 K. Note that the ordinate for the CO_2 desorption spectra has been expanded by a factor of 50 relative to that in the CO desorption spectra.

planes of Rh single crystals (16, 18, 19). A small fraction of the adsorbed CO was oxidized to CO_2, which desorbed in a broad peak centered at 500 K, as shown in the lower portion of Fig. 5. This result is consistent with previous studies of Rh supported on polycrystalline CeO_2 (8, 9, 18). In those studies the production of CO_2 was attributed to the migration of oxygen from the oxide lattice onto the supported Rh and its subsequent reaction with CO. A major difference between the present work and the studies employing polycrystalline substrates, however, is the amount of CO_2 which was produced. In the present study, less than 2% of the adsorbed CO was oxidized to CO_2, while for Rh on polycrystalline CeO_2 this value was as high as 20% (9).

The remaining spectra in Fig. 5 demonstrate the effect of heating the Rh/CeO_2(111) sample to a series of higher temperatures on the CO TPD results. The most noticeable change with increasing pretreatment temperature was a decrease in the intensity of the desorption peaks for both CO and CO_2. A slight decrease in the desorption temperatures for both CO and CO_2 also occurred as the annealing temperature was increased. As shown in Fig. 6, the area of the CO peak decreased nearly linearly with temperature. The

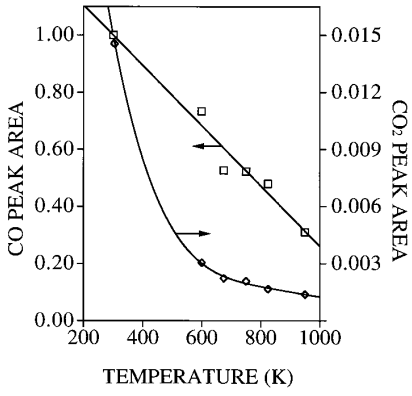

FIG. 6. CO, (□) and CO_2 (◇) TPD peak areas as a function of sample pretreatment temperature. The CO and CO_2 peak areas were normalized to the CO peak area from the as-deposited film.

area of the CO peak obtained from a sample previously heated to 950 K was 30% of that obtained from the as-deposited Rh film. In contrast, the decrease in the area of the CO_2 peak was nonlinear and occurred more rapidly than that of CO, decreasing by 80% after heating to only 600 K. Smaller decreases in area were observed after annealing to higher temperatures. AES spectra collected following the TPD experiments did not show any surface carbon. Thus, the decrease in the peak areas is a result of a reduction in Rh surface area and is consistent with the AES experiments which showed that the Rh layer agglomerates upon heating. In addition to the data shown in Fig. 5 for a 3 ML Rh film, similar sets of experiments were performed for Rh coverages of 0.5 and 1.5 ML. The results obtained for these coverages were qualitatively similar to those of the 3 ML film.

A closer examination of the data in Fig. 5 reveals that in addition to the CO desorption feature at 500 K, there is a small CO peak centered at 600 K. The area of this high-temperature CO peak was always less than 15% of that of the primary CO peak. It is interesting that the small CO desorption feature is at a temperature significantly higher than that reported for CO desorption from Rh single crystals and foils (16–19). A quantitative analysis of the data in Fig. 5 can also be used to obtain an estimate of the average Rh particle size. Comparison of the CO peak areas to that obtained for saturation coverage of CO on a continuous metal film allowed the amount of CO adsorbed on the model catalysts to be estimated. Assuming spherical Rh particles and one adsorbed CO per surface Rh atom, the average diameter for the as-deposited 3 ML Rh layer was estimated to be 25 Å. Annealing to 950 K caused the average particle size to increase to 95 Å.

In order to investigate the effect surface reduction has on the Rh–CeO_2 interaction, experiments were performed on CeO_2(111) samples which had been slightly reduced by lightly sputtering with Ar^+ ions prior to deposition of the Rh film. Figure 7 displays a series of CO TPD spectra obtained from a 1.5 ML Rh film deposited on a CeO_2(111) substrate that had been sputtered for 15 min with 500 eV Ar^+ ions. The top spectrum in this figure corresponds to the as-deposited film, while the remaining spectra were obtained after heating the sample to the indicated temperatures. These spectra again exhibit two CO desorption features centered near 500 and 600 K. The high-temperature CO peak is much more pronounced, however, than those in the data obtained from the oxygen-annealed CeO_2(111) substrate. For samples heated to temperatures less than 600 K, the ratio of the intensities of the low and high-temperature CO peaks was nearly 1 : 1. Briefly heating the Rh/CeO_2 sample to higher temperatures resulted in a reduction in the intensity of both CO desorption features and a slight decrease in the desorption temperatures. The intensity of the high-temperature peak, however, was found to decrease more rapidly than that of the low-temperature peak. The ratio of the areas of the low and high-temperature CO peaks as a function of the sample annealing temperature is displayed in Fig. 8. The bottom curve in Fig. 7 was obtained after annealing the sample at 950 K for 20 min. Only the low-temperature CO desorption feature, now centered at 480 K, was observed in this spectrum.

Small amounts of CO_2 were also detected during TPD experiments employing the sputtered CeO_2(111) surface. Carbon dioxide was found to desorb in a broad peak located between 500 and 600 K. In all cases, the amount of adsorbed CO oxidized to CO_2 was less than 2%.

The reaction of CO on 1.5 ML of Rh supported on the CeO_2(100) substrate was also examined using TPD. Figures 9a and 9b illustrate the CO and CO_2 desorption spectra for Rh supported on a (100) thin film annealed in oxygen and in vacuum, respectively. These TPD results are similar to those obtained from the CeO_2(111) surface, and exhibit both a

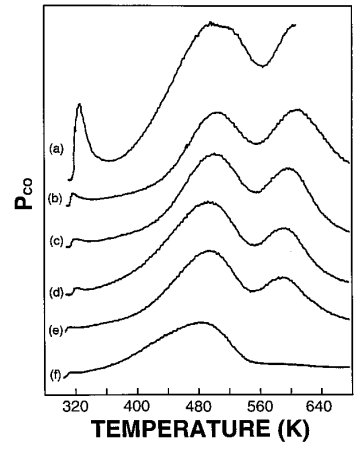

FIG. 7. TPD spectra following CO adsorption at 300 K on the 1.5 ML Rh film supported on sputtered CeO_2(111) for pretreatment temperatures of (a) 300, (b) 600, (c) 750, (d) 900, (e) 950, and (f) 950 K.

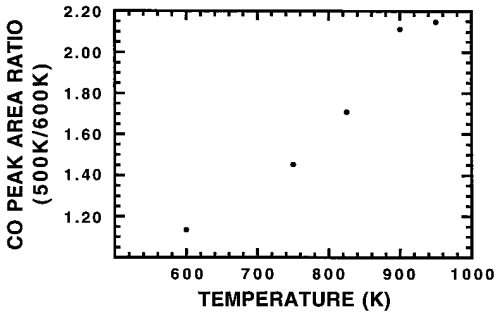

FIG. 8. Peak area ratio of the low to high-temperature CO desorption features as a function of pretreatment temperature.

low- and high-temperature CO desorption peak and a less than 2% conversion of CO to CO_2. The high-temperature CO feature was much more pronounced in the spectrum from the vacuum-annealed surface relative to that from the oxygen-annealed surface. This result suggests that annealing of the CeO_2(100) film in vacuum was sufficient to partially reduce the surface.

DISCUSSION

The experimental results indicate that both the CeO_2(111) and CeO_2(100) surfaces are not very effective in stabilizing the dispersion of supported Rh. Rh films deposited at 300 K were found to grow via the formation of three-dimensional particles rather than in a layer-by-layer fashion. The Rh particles formed at room temperature underwent further agglomeration upon heating. This result is somewhat surprising in light of previous studies which have suggested that the addition of CeO_2 to three-way automotive catalysts results in stabilization of noble metal dispersion (2–6).

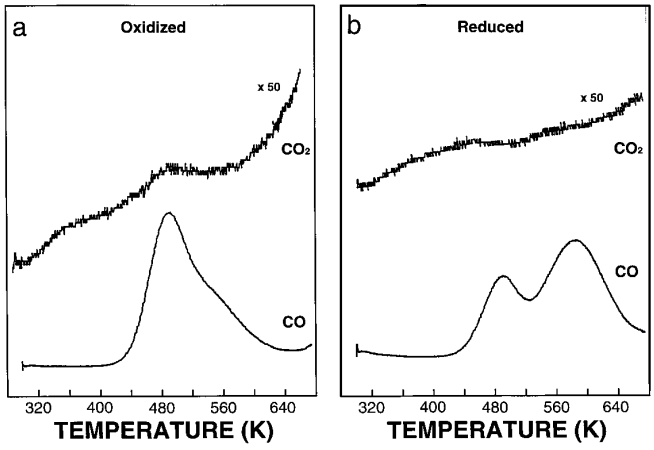

FIG. 9. TPD spectra following CO adsorption at 300 K on a 1.5 ML Rh film supported on (a) the oxidized CeO_2(100) sample and (b) the vacuum-annealed CeO_2(100) sample.

A fraction of the CO adsorbed on Rh/CeO_2(111) and Rh/CeO_2(100) was oxidized to CO_2, as shown in Figs. 5 and 9a. One possible explanation for this result is that a small amount of oxygen from the background gas in the chamber adsorbed on the metal particles. However, in experiments in which CO and O_2 were intentionally coadsorbed, CO_2 was produced at 400 K. This is 100 K lower than the CO_2 desorption temperature from the samples exposed only to CO. Thus, adsorption of O_2 from the background cannot be responsible for the CO_2 production. Another possibility is that a portion of the CO adsorbs dissociatively. The lack of carbon deposition following the TPD experiments, however, rules out this possibility. The most likely explanation is that the oxygen came from the CeO_2 lattice. This conclusion is consistent with the study of Zafiris and Gorte on the interaction of CO with Rh supported on polycrystalline CeO_2 (8, 9). In that study, a fraction of the adsorbed CO was also found to be oxidized to CO_2 at a temperature substantially higher than that when oxygen and CO were coadsorbed. Zafiris and Gorte attributed the production of CO_2 to the migration of oxygen from the CeO_2 lattice onto the supported Rh particles at temperatures above 400 K.

Although the results obtained for Rh supported on the CeO_2 single-crystal surfaces and on polycrystalline CeO_2 have similar features, they differ in regard to the fraction of adsorbed CO which is oxidized to CO_2. In the present study, less than 2% of the adsorbed CO desorbs as CO_2, while in the case of Rh supported on polycrystalline CeO_2, this value is as high as 20% (9). This result demonstrates that the structure of the CeO_2 influences the rate of oxygen transfer from the support to the Rh particles. A nonisotropic diffusivity for oxygen ions in the CeO_2 lattice is one possible explanation for this structure sensitivity. If this is the case, the rate of oxygen migration from CeO_2 to supported Rh may depend on the crystallographic orientation of the oxide surface. This does not appear to be the primary constraint, however, as evidenced by the similarity in the amount of CO oxidation obtained from Rh supported on both the CeO_2(100) and CeO_2(111) surfaces. Another possibility is that there are mechanisms for oxygen diffusion in polycrystalline CeO_2 that are not available in the single crystal samples. For example, grain boundary diffusion may play an important role in oxygen transport in the polycrystalline support.

The data in Figs. 5 and 6 demonstrate that changes in the morphology of the supported Rh particles, which occur upon heating, influence the percentage of adsorbed CO which is oxidized to CO_2. For the as-deposited Rh film, the ratio of CO_2 to CO in the TPD spectra was 0.015. After heating to 600 K, this ratio decreased to 0.004. Heating the Rh/CeO_2(111) sample to higher temperatures produced smaller changes in the CO_2/CO ratio. After heating to 950 K, the CO_2/CO ratio was 0.0035. Since oxygen is being supplied by the CeO_2(111) support, the most likely

explanation for the change in the CO_2/CO ratio with sample annealing temperature is that only CO molecules adsorbed at or near the Rh–CeO_2(111) interface are involved in the oxidation reaction. The ratio of the number of exposed Rh atoms at the Rh–CeO_2(111) interface to the total number of exposed Rh atoms would be a nonlinear function of the Rh particle size, with small particles having a higher percentage of atoms at the interface. This scenario is consistent with the data described above which shows that the percentage of CO oxidized to CO_2 was highest on the as-deposited Rh film which was composed of the smallest Rh particles.

The most interesting observation of this study was the effect reduction of the CeO_2 single-crystal surfaces had on the interaction of CO with the supported Rh particles. Partial reduction of the CeO_2(111) and CeO_2(100) surfaces resulted in the stabilization of a fraction of the CO molecules adsorbed on the supported Rh layer. The CO TPD spectra obtained from partially reduced samples exhibited two CO desorption features, a low-temperature peak located at 500 K, corresponding to CO desorption from bulk Rh, and a high-temperature peak centered at 600 K. For Rh films on the freshly sputtered (111) surface, the high-temperature CO desorption feature was larger than the low-temperature feature. The high-temperature peak decreased in intensity, however, relative to low-temperature peak as the sample was annealed to higher temperatures. The XPS results showed that reoxidation of the sputtered CeO_2(111) surface occurred upon annealing in vacuum. This is typical of macroscopic metal oxide single crystals in UHV (24) and can be explained by diffusion of oxygen from the bulk to the crystal surface. Hence, the area of the high-temperature CO peak can be related to the concentration of Ce^{+3} cations (or degree of reduction) in the surface region of the oxide. Although small, the high-temperature CO desorption feature was also present in the TPD spectra obtained from Rh films supported on oxygen-annealed CeO_2(111). This result suggests that the annealed surfaces were not fully oxidized. This is not surprising since these surfaces would be expected to contain a small number of oxygen vacancies and Ce^{+3} cations. In the case of the CeO_2(100) thin film, both the XPS and TPD results indicated a relatively high population of Ce^{+3} cations on the oxygen-annealed surface. The TPD results further indicated that heating in vacuum was sufficient to partially reduce the CeO_2(100) thin film.

Although it is apparent that CO adsorbed on Rh associated with reduced portions of the CeO_2(111) and CeO_2(100) surfaces is significantly stabilized relative to CO adsorbed on bulk Rh, the mechanism by which this stabilization occurs cannot be deduced from the results of this investigation. Previous studies, however, may provide a clue as to the nature of this interaction. In an FTIR study of the interaction of CO with Rh/CeO_2/SiO_2, Kiennemann *et al.* observed that in addition to peaks characteristic of the ν(CO) mode of CO adsorbed on the low index planes of Rh, the FTIR spectra contained a low-frequency ν(CO) peak centered at 1725 cm^{-1} (12). Based on comparisons to the IR spectra of known metal carbonyl compounds, this peak was ascribed to an adsorbed CO species in which the carbon end of the molecule is bound to Rh and the oxygen end interacts with a cerium cation of the support. Similar results were obtained by Lavalley *et al.* for the interaction of CO with Rh/CeO_2 (25). Since the catalysts used by these researchers were highly reduced (as determined by XPS), the low-frequency CO stretching mode was attributed to CO bridged between Rh and a surface Ce^{+3} cation. Lööf *et al.* have also reported that reduced ceria stabilizes the interaction of CO with Rh (10). These results suggest that the high-temperature CO desorption state observed in the present study may result from the desorption of CO which is bridge bonded between Rh and Ce^{+3} cations on the CeO_2 support. We are currently exploring this possibility by using HREELS to characterize the vibrational spectrum of CO adsorbed on Rh/CeO_2(111) model catalysts.

CONCLUSIONS

Rhodium films on CeO_2(111) and CeO_2(100) were found to undergo three-dimensional particle growth for a substrate temperature of 300 K. Annealing to temperatures in excess of 600 K resulted in further agglomeration of the Rh layer. Carbon monoxide desorption spectra obtained from the Rh films were similar to those which have been obtained previously for the low-index planes of Rh. A small fraction of the CO adsorbed on the Rh/CeO_2(111) and RhCeO_2(100) samples was found to be oxidized to CO_2 during TPD experiments, with the oxygen being supplied by the oxide support. The faster decrease in the CO_2 peak area relative to that of CO with increasing particle size indicates that the oxidation reaction occurred at the Rh–CeO_2 interface. Differences in the fraction of adsorbed CO which is oxidized to CO_2 for Rh supported on CeO_2(111) and CeO_2(100) relative to polycrystalline CeO_2, indicates that the migration of oxygen from CeO_2 to Rh is structure sensitive.

Partial reduction of the CeO_2(111) and CeO_2(100) substrates was found to influence the interaction of CO with the supported Rh. A fraction of the CO adsorbed on Rh particles supported on partially reduced CeO_2 single-crystal surfaces was stabilized and desorbed at a temperature 100 K higher than that for CO adsorbed on bulk Rh. The stabilization of the adsorbed CO was found to correlate with the presence of Ce^{+3} cations on the surface of the CeO_2(111) and CeO_2(100) supports.

ACKNOWLEDGMENTS

We thank Ray Gorte and Georgios Zafiris for many helpful comments and suggestions throughout the course of this study. We also acknowledge Dr. Eric Brosha and Dr. Fernando Garzon of Los Alamos National Laboratory for kindly providing the CeO_2(100) sample. This work was

supported by the National Science Foundation through the NSF-MRL program (Grant DMR91-20668).

REFERENCES

1. Schlatter, J., and Taylor, K., *J. Catal.* **49**, 42 (1977).
2. Duplan, J. L., and Praliaud, H., *Appl. Catal.* **67**, 325 (1991).
3. Harrison, B., Diwell, A. F., and Hallett, C., *Platinum Metals Rev.* **32**, 73 (1988).
4. Su, E. C., Montreuil, C. N., and Rothschild, W. G., *Appl. Catal.* **17**, 75 (1985).
5. Su, E. C., and Rothschild, W. G., *J. Catal.* **99**, 506 (1986).
6. Taylor, K. C., *Chemtech* **20**, 551 (1990).
7. Dictor, R., and Roberts, S., *J. Phys. Chem.* **93**, 5846 (1989).
8. Zafiris, G. S., and Gorte, R. J., *J. Catal.* **143**, 86 (1993).
9. Zafiris, G. S., and Gorte, R. J., *J. Catal.* **139**, 561 (1993).
10. Lööf, P., Kasemo, B., Andersson, S., and Frestad, A., *J. Catal.* **130**, 181 (1991).
11. Laachir, A., Perrichon, V., Bernal, S., Calvino, J. J., and Cifredo, G. A., *J. Molec. Catal.* **89**, 391 (1994).
12. Kiennemann, A., Breault, R., and Hindermann, J. P., *J. Chem. Soc. Faraday Trans. 1* **83**, 2119 (1987).
13. Warren, J. P., Zhang, X., Andersen, J. E. T., and Lambert, R. M., *Surf. Sci.* **287/288**, 222 (1993).
14. Belton, D. N., and Schmieg, S. J., *J. Vac. Sci. Technol.* **11**, 2330 (1993).
15. Peden, C. H. F., and Houston, J. E., *J. Catal.* **128**, 405 (1991)
16. Baird, R. J., Ku, R. C., and Wynblatt, P., *Surf. Sci.* **97**, 346 (1980).
17. Gorodetskii, V. V., and Nieuwenhuys, B. E., *Surf. Sci.* **105**, 299 (1981).
18. Marbrow, R. A., and Lambert, R. M., *Surf. Sci.* **67**, 489 (1977).
19. Thiel, P. A., Williams, E. D., Yates, J. T., and Weinberg, W. H., *Surf. Sci.* **84**, 54 (1979).
20. Shyu, J. Z., Weber, W. H., and Gandhi, H. S., *J. Phys. Chem.* **92**, 4964 (1988).
21. Creaser, D. A., Harrison, P. G., Morris, M. A., and Wolfindale, B. A., *Catal. Lett.* **23**, 13 (1994).
22. Stubenrauch, J., and Vohs, J. M., unpublished results.
23. Zafiris, G. S., Ph.D. thesis, University of Pennsylvania, 1993.
24. Kim, K. S., and Barteau, M. A., *J. Catal.* **125**, 353 (1990).
25. Lavalley, J. C., Saussey, J., Lamotte, J., Breault, R., Hindermann, J. P., and Kiennemann, A., *J. Phys. Chem.* **94**, 5941 (1990).